



UNIVERSITÀ POLITECNICA DELLE MARCHE
Repository ISTITUZIONALE

Optimal error governor for PID controllers

This is the peer reviewed version of the following article:

Original

Optimal error governor for PID controllers / Cavanini, L; Ferracuti, F; Monteriu, A. - In: INTERNATIONAL JOURNAL OF SYSTEMS SCIENCE. - ISSN 0020-7721. - 52:12(2021), pp. 2480-2492. [10.1080/00207721.2021.1890272]

Availability:

This version is available at: 11566/289811 since: 2024-04-25T09:50:08Z

Publisher:

Published

DOI:10.1080/00207721.2021.1890272

Terms of use:

The terms and conditions for the reuse of this version of the manuscript are specified in the publishing policy. The use of copyrighted works requires the consent of the rights' holder (author or publisher). Works made available under a Creative Commons license or a Publisher's custom-made license can be used according to the terms and conditions contained therein. See editor's website for further information and terms and conditions.

This item was downloaded from IRIS Università Politecnica delle Marche (<https://iris.univpm.it>). When citing, please refer to the published version.

(Article begins on next page)

Optimal Error Governor for PID controllers

Luca Cavanini¹ and Francesco Ferracuti² and Andrea Monteriù²

¹Industrial Systems and Control Ltd, Culzean House, 36 Renfield Street, Glasgow G2 1LU, UK; ²Università Politecnica delle Marche, Via Brecce Bianche 12, 60131 Ancona

ARTICLE HISTORY

Compiled April 25, 2024

ABSTRACT

Error Governor (EG) deals with the problem of dynamically modifying the feedback error driving a controller having bounded control signals, for preventing controller or actuators saturation, avoiding integrator and/or slow dynamics windup and preserving the nominal linear controller behaviour. In this paper, an optimization-based EG scheme is proposed for discrete-time Proportional-Integral-Derivative (PID) controllers driving Single-Input Single-Output (SISO) plants. The PID controller is considered in state-space form and this formulation is used to pose the EG problem as a constrained quadratic program (QP). Because the QP problem is subject to inequality constraints related to controller saturation, in order to use the proposed scheme in real-world applications, it should be necessary to consider appropriate algorithms for efficiently solving the optimization problem. An efficient way to efficiently compute the solution of the EG problem is presented, reducing the computational effort required to solve the EG QP for using the proposed scheme in real control loops with high sampling rate. An analysis of control performance and computational burden is provided, comparing in simulation studies the optimal EG scheme performance with respect to control results provided by saturated PID with and without anti-windup action.

KEYWORDS

Error governor; PID; Anti-windup; SISO

1. Introduction

Proportional-Integrative-Derivative (PID) controllers are used in a wide range of fields, e.g. process control and power converters, micro-manipulation and aerospace. PID algorithms are present in different forms in more than 90% of the over-all control loops developed (Åström & Hägglund, 2001), as standard single-loop controllers or as part of hierarchical, programmable or distributed control systems (Cavanini, Cimini, Ippoliti, & Bemporad, 2017; Cavanini, Colombo, Ippoliti, & Orlando, 2017; Shi & Yang, 2018; Song, Huang, & Wen, 2017). Despite the advanced control technology development of the last twenty years, PID still remains the most popular approach, due to the simple structure, conceptually easy to understand and providing adequate performance in the vast majority of applications (Liu & Daley, 2001). In fact, the three terms defining the PID control law fulfill the three most common required control performance: the proportional term provides a fast response to the actual error value, without guaranteeing

a good steady-state accuracy; the integral term, providing a slower response, yields the steady-state zero error and rejection of constant disturbances; the derivative term addresses fast error dynamics, and is usually used in conjunction with filters to limit sensor noise effects (in this case the controller is usually indicated as PIDF) (Knospe, 2006).

A key factor of the PID success is also related to the fact this controller is easy to tune. The straightforward ZieglerNichols (Z-N) empirical tuning approach and the frequency response analysis are classical but still the most common methods used for PID tuning (Ang, Chong, & Li, 2005). Furthermore, several automatic PID tuning algorithms have been proposed from the standard relay auto-tuning, used in process control, to the most advanced solution (Berner, Soltesz, Hägglund, & Åström, 2018). Overall tuning methods are based on a common assumption: the standard PID controller is a linear time-invariant (LTI) system, proving a control effort changing linearly with the feedback error all-over the operating conditions of the controlled system. Of course, PID tuning parameters can be modified (e.g. by switching or gain scheduling policies (Chaiyatham & Ngamroo, 2017; Wang, Xiao, Liu, & Liu, 2015)) according to the plant dynamics knowledge, overlaying limits related to particular control scenarios or plant configurations. By the way, a unified solution to most common PID design issues is still subject of research (Azar & Serrano, 2015; Berner, Soltesz, Åström, & Hägglund, 2017; Mercader, Åström, Banos, & Hägglund, 2017).

In this paper, the authors propose an Error Governor (EG) scheme for improving the control performance of discrete-time PID controllers with control input saturation. PID controllers with anti-windup strategies represent a wide part of PID algorithms in digital control systems and worth investigation for their spread application in different fields (Izadbakhsh, Kalat, Fateh, & Rafiei, 2011; Izadbakhsh & Kheirkhahan, 2018; Izadbakhsh & Kheirkhahan, 2018). Governor policies are add-on modules for introducing constraints on plant and controller signals in pre-compensated closed-loop schemes, improving the control performance provided by the primal controller driving the considered system. The most widely used, and famous, governor paradigm is the Reference Governor (RG) (Kolmanovsky, Garone, & Di Cairano, 2014), also named Command Governor (CG) (Garone, Di Cairano, & Kolmanovsky, 2017). As its name suggests, the RG is an add-on scheme for enforcing pointwise-in-time state and control constraints by modifying the reference command to a well-designed (for small signals) closed-loop system. Different command governor schemes have been proposed in the last years, e.g. scalar and vector reference governors, extended command governors, incremental reference governors, feed-forward reference governors, network reference governors, reduced order reference governors, parameter governors, virtual state governors (Angeli & Mosca, 1999; Bemporad, 1998; Casavola, Franzè, Menniti, & Sorrentino, 2011; Cavanini, Cimini, & Ippoliti, 2016; Cavanini, Cimini, Ippoliti, & Bemporad, 2017). The objective of the different governor policies is to preserve, or improve, the response of the closed-loop system designed by conventional control techniques. Usually, RG achieves this by ensuring that the modified reference command is as close as possible to the original set-point signal subject to satisfying a set of provided constraints (Garone et al., 2017).

Close in spirit to command governors, EG is a control paradigm initially proposed for continuous-time controllers (Kapasouris, Athans, & Stein, 1988), recently considered in conjunction with adaptive control laws for aerospace applications (Kahveci & Kolmanovsky, 2010; Tharayil & Alleyne, 2002). The aim of EG is to avoid controller output signal saturation and integrator windup on limited power control boards by managing the feedback error signal (Kapasouris et al., 1988). Despite the sensible

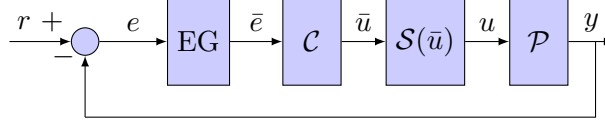


Figure 1. Closed-loop system with error governor for input saturated system

problems of controllers faced by EG, in particular for PID control systems, it has been not studied in detail in the last years.

This paper presents an optimal approach to the EG scheme design for PID controllers driving SISO plants. The controller is considered in the discrete-time state-space form, and it is used for formulating a quadratic cost function subject to a set of convex linear constraints defining the EG constrained optimization problem. The optimization problem is cast in a Quadratic Programming (QP) condensed form, which is possible to solve by the most common algorithms (Ferreau et al., 2017). Furthermore, an algorithm is proposed to efficiently compute the solution of the QP problem, avoiding the use of on-line computationally expensive QP solvers (Cavanini, Cimini, & Ippoliti, 2017). The proposed method permits to *i*) maintain the standard PID formulation, whereas some standard windup schemes require changes in the control law, *ii*) compensate the windup issue affecting PID controllers, *iii*) avoid control action saturation. Furthermore, the efficient form of the proposed EG permits to apply the add-on in provided closed-loop systems featured by fast control rates. The proposed EG has been compared in simulation tests, with respect to standard saturated PID, with and without the anti-windup action, comparing control performance and computational burden.

The paper is organized as follows. In section 2, the EG problem for discrete-time controllers is presented. In section 3, the proposed optimal EG is given, reporting QP formulation and the proposed algorithm for efficiently computing the solution of the optimization problem. In section 4, simulation results are presented, comparing different PID controllers with the proposed method. Section 5 concludes the paper.

2. SISO Error Governor Problem

In this section the Error Governor problem for SISO systems is presented. Referring to the control scheme shown in Figure 1, a SISO discrete time linear plant \mathcal{P} is considered

$$\begin{aligned} x(k+1) &= A_p x(k) + B_p u(k) \\ y(k) &= C_p x(k) \end{aligned} \quad (1)$$

where $x \in \mathbb{R}^{n_x}$ is the plant state vector, $y \in \mathbb{R}^{n_y}$, is the output signal, $u \in \mathbb{R}^{n_u}$, is the input signal, $A_p \in \mathbb{R}^{n_x \times n_x}$, $B_p \in \mathbb{R}^{n_x \times n_u}$ and $C_p \in \mathbb{R}^{n_y \times n_x}$ are the plant state-space matrices. In the case of SISO plant, it is supposed to be $n_y=1$ and $n_u=1$. A non-linearity saturation is imposed on the control input u , such that the plant control input belongs to an admissible control input set \mathbb{U} defined as:

$$\mathbb{U} = \{u \in \mathbb{R}^{n_u} | \bar{u}_m \leq u \leq \bar{u}_M\}, \quad (2)$$

with $\bar{u} \in \mathbb{R}^{n_u}$ the unsaturated control signal and $u \in \mathbb{U} \subset \mathbb{R}^{n_u}$ is the constrained control input vector bounded according to the saturation function $\mathcal{S}(\bar{u}) : \mathbb{R}^{n_u} \rightarrow \mathbb{R}^{n_u}$ defined as

$$u = \mathcal{S}(\bar{u}) = \begin{cases} \bar{u} & \text{if } \bar{u}_m \leq \bar{u} \leq \bar{u}_M, \\ \bar{u}_m & \text{if } \bar{u} < \bar{u}_m, \\ \bar{u}_M & \text{if } \bar{u} > \bar{u}_M, \end{cases} \quad (3)$$

where \bar{u}_m and \bar{u}_M are the minimum and maximum admissible control input bounds, respectively. The controller \mathcal{C} is considered in discrete-time state-space form

$$\begin{aligned} x_c(k+1) &= A_c x_c(k) + B_c \bar{e}(k) \\ \bar{u}(k) &= C_c x_c(k) + D_c \bar{e}(k) \end{aligned} \quad (4)$$

where $A_c \in \mathbb{R}^{n_{x_c} \times n_{x_c}}$, $B_c \in \mathbb{R}^{n_{x_c} \times n_y}$, $C_c \in \mathbb{R}^{n_{\bar{u}} \times n_{x_c}}$ and $D_c \in \mathbb{R}^{n_{\bar{u}} \times n_y}$ are the controller state-space matrices, $x_c \in \mathbb{R}^{n_{x_c}}$ is the controller state vector and $\bar{e} \in \mathbb{R}^{n_y}$ is the feedback error driving the controller. In the case of SISO plant, it is supposed to be $n_y=1$ and $n_{\bar{u}}=1$. The objective of the controller \mathcal{C} is to set to zero the feedback tracking error $e(k) = r(k) - y(k)$, for a constant reference signal $r \in \mathbb{R}^{n_y}$ consistent with the feasible steady-state set-points of the plant, $y(k) = y(t)|_{t=kT_s}$ the controlled output and with T_s the controller sample time.

Remark 1. The closed loop system given by the SISO plant \mathcal{P} driven by the feedback controller \mathcal{C} in presence of input saturation \mathcal{S} is stable.

When a linear plant \mathcal{P} without input bounds is considered, the control objective can be achieved by standard techniques, because EG is not required and $e(k) = \bar{e}(k)$. In presence of input saturation the tracking result can be improved introducing an EG policy in the feedback loop (Kapasouris et al., 1988) designed by classical control methods. The objective of the EG is managing the commanded error $\bar{e}(k) \in \mathbb{R}^{n_y}$ minimizing the change with respect to the real error $e(k)$, guaranteeing the controller control signal \bar{u} belongs to the set defined as in Eq. (2), such that $u(k) = \mathcal{S}(\bar{u}(k)) = \bar{u}(k)$, avoiding windup and improving the closed loop performance (Kapasouris et al., 1988).

3. Optimal Error Governor for PID Controller

In this section, the proposed optimal approach to EG for PID controllers is presented. The PID is considered in state-space form and the optimal EG is formulated according. Then the efficient solution of the EG problem is shown.

3.1. PID state-space model

Here the discrete-time state-space representation of the PID controller is given.

Definition 3.1. Consider the parallel formulation of a discrete-time PID controller

and backward Euler formula for integration and derivative filter

$$\frac{\bar{U}(q)}{\bar{E}(q)} = K_p + K_i T_s \frac{1}{1-q} + K_d \frac{\delta}{1 + \delta T_s \frac{1}{1-q}} \quad (5)$$

where $q = z^{-1}$, K_p , K_i and K_d are the proportional, integral and derivative gains, respectively, T_s is the sampling time, $\delta = \frac{1}{t_f}$ is the derivative filtering term, $\bar{e}(k)$ is the provided error between the reference and the actual measure and \bar{u} is the control signal. The discrete-time state-space representation of Eq. (5) will be denoted by $\mathcal{C}(A_c, B_c, C_c, D_c)$, and corresponds to:

$$\begin{aligned} x_c(k+1) &= \underbrace{\begin{bmatrix} 1 & 0 \\ 0 & \alpha \end{bmatrix}}_{A_c} x_c(k) + \underbrace{\begin{bmatrix} \tilde{K}_i \\ -\tilde{K}_d(1-\alpha) \end{bmatrix}}_{B_c} \bar{e}(k) \\ \bar{u}(k) &= \underbrace{\begin{bmatrix} 1 & 1 \end{bmatrix}}_{C_c} x_c(k) + \underbrace{\begin{bmatrix} K_p + \tilde{K}_i + \tilde{K}_d \end{bmatrix}}_{D_c} \bar{e}(k) \end{aligned} \quad (6)$$

with

$$\tilde{K}_i = K_i T_s \quad , \quad \tilde{K}_d = \frac{K_d}{T_s + t_f} \quad , \quad \alpha = \frac{t_f}{t_f + T_s}. \quad (7)$$

Definition 3.1 presents the state-space representation of the discrete-time PID controller in parallel form. Eq. (6) shows state-space matrices of the PID are featured by a state vector of size $n_{x_c} = 2$, where $x_c(k) = [x_{c(i)}(k) \ x_{c(d)}(k)]'$, such that $x_{c(i)}(k)$ represents the internal state of the controller related to the integral action, and $x_{c(d)}(k)$ is the state variable related to the derivative term. Note that, when an only proportional controller is considered, the control signal is given by $\bar{u}(k) = D_c \bar{e}(k) = K_p \bar{e}(k)$. A wide set of PID formulations can be found in literature and real-world applications. The different forms of PID controllers (e.g. series and ideal) can always be cast to the parallel form (Åström & Hägglund, 1995), presented in Definition 3.1 that will be considered in the following.

3.2. Optimal error governor

The proposed method considers computing the managed error \bar{e} by minimizing the following quadratic cost function subject to affine constraints

$$\min_{\bar{e}} \quad \|e(k) - \bar{e}(k)\|_2^2 \quad (8a)$$

$$\text{s.t.} \quad \bar{u}(k) = C_c x_c(k) + D_c \bar{e}(k) \quad (8b)$$

$$\bar{u}(k) \in \mathbb{U} \quad (8c)$$

where $e(k)$ is the feedback error value at the time instant k , $\bar{e}(k)$ is the managed error representing the optimization variable to compute for finding the cost function minimum value and \mathbb{U} is the convex set of constraints on the control signal \bar{u} from Eq. (2). Note that only the output equation of the controller model is considered imposing equality constraints in Eq. (8b). The problem of Eq. (8) can be cast in the

following condensed form of the QP problem, aided to be solved by the most common algorithms

$$\begin{aligned} \min_z \quad & \frac{1}{2} z' H z + \rho_k' F' z \\ \text{s.t.} \quad & G z \leq W \rho_k + w \end{aligned} \quad (9)$$

where $H = 1$ is the Hessian term, $F = [-1 \ 0 \ 0]$ is the linear term, $\rho_k = [e(k) \ x_{c(i)}(k) \ x_{c(d)}(k)]'$ is the vector of time-varying parameters, z is the optimization variable, such that the optimal solution is $z^* = \bar{e}^*(k)$, and the constraints matrices are

$$G = \begin{bmatrix} D_c \\ -D_c \end{bmatrix}, \quad W = \begin{bmatrix} 0 & -C_c \\ 0 & C_c \end{bmatrix}, \quad w = \begin{bmatrix} \bar{u}_M \\ -\bar{u}_m \end{bmatrix}. \quad (10)$$

Under the stability assumption of Remark 1, the formulation of the EG problem presented in Sec. 2 permits to compute the managed error $\bar{e}(k)$ minimizing the l_2 norm difference with respect to the original feedback error $e(k)$, satisfying the convex constraints which guarantee to avoid the control input saturation of the output constrained PID controller. In order to compute the solution of the QP problem of Eq. (9) it is required the introduction of appropriate algorithms, permitting to efficiently solve the constrained optimization problem (Cimini & Bemporad, 2019). In fast dynamics closed-loop systems, featured by high sampling rates or reduced computational power, complex QP solver algorithms can be too computationally expensive for computing on-line the solution of the EG optimal problem. In order to address this issue, in the following an efficient approach for computing the solution of the optimal QP EG problem is presented.

3.3. Efficient solution

The following result resumes the computation of the efficient solution of the optimization problem of Eq. (8).

Lemma 3.1. *Considering the PID state-space representation Eq. (6), the optimal solution $\bar{e}^*(k)$ of the EG problem formulated as in Eq. (8) is given by*

$$\bar{e}^*(k) = \frac{\hat{u}(k)}{D_c} - C_c x_c(k) \frac{1}{D_c} \quad (11)$$

where $\hat{u}(k)$ is computed by the saturation function of Eq. (3), defined with respect to the PID output bounds \bar{u}_m and \bar{u}_M , with $\bar{u}_m < \bar{u}_M$, such that $\hat{u}(k) = \mathcal{S}(C_c x_c(k) + D_c e(k))$.

Proof 1. The optimality of the solution $\bar{e}^*(k)$ computed by Eq. (11) is proved studying the possible values of $\hat{u}(k)$:

- i) if $\mathcal{S}(C_c x_c(k) + D_c e(k)) \in \mathbb{U}$ then $\hat{u}(k) = \bar{u}(k)$ and the optimization variable is

$$\begin{aligned} \bar{e}^*(k) &= \frac{\bar{u}(k)}{D_c} - C_c x_c(k) \frac{1}{D_c} = \\ &= [C_c x_c(k) + D_c e(k)] \frac{1}{D_c} - C_c x_c(k) \frac{1}{D_c} = e(k) \end{aligned} \quad (12)$$

such that the cost function value is zero.

- ii) if $\mathcal{S}(C_c x_c(k) + D_c e(k)) \notin \mathbb{U}$, then $\hat{u}(k) = \bar{u}_M$ or $\hat{u}(k) = \bar{u}_m$. For $\hat{u}(k) = \bar{u}_M$, the constraint on the maximum value of the control effort signal $\bar{u}(k)$ is active, such that

$$\bar{u}_M = C_c x_c(k) + D_c \bar{e}^*(k) \quad (13)$$

Inverting Eq. (13), $\bar{e}^*(k)$ is computed according to Eq. (11). The same approach is used if $\hat{u}(k) = \bar{u}_m$, when control signal constraint on minimum is active.

Lemma 3.1 provides an efficient solution of the EG problem formulated in Eq. (8). By the efficient solution, the EG policy initially formulated as a constrained optimization problem, expensive to solve in terms of time and computational burden, can be computed by a reduced set of algebraic operations in an efficient way. This form of the EG suggests that the proposed policy can be introduced also in fast dynamics closed loops, driven by simple PID controllers with saturation.

3.4. Anti-windup action

The effects of saturation are noticeable when the controller is an unstable system. This is always the case for a controller with integral action. Since the feedback loop is broken when the actuator saturates, the unstable modes of the regulator may then drift to undesirable values. The consequences are that it may take a long time for the system to reach equilibrium after an upset. The phenomenon which was first noticed in conventional PID control is therefore called integrator windup (Astrom & Rundqwist, 1989). The introduced EG algorithm provides a direct anti-windup action, by changing the PID feedback error. When the managed error has the same value of the original feedback error $\bar{e}(k) = e(k)$, the PID state vector evolves according to the nominal PID model of Eq. (4) and the controller operates according to the design linear law. Furthermore, when the EG provides a governed error $\bar{e}(k) \neq e(k)$, the original PID model is driven by an error $\bar{e}(k)$ computed according to Eq. (11), such that

$$x_c(k+1) = A_c x_c(k) + B_c \left(\frac{\hat{u}(k)}{D_c} - \frac{C_c x_c(k)}{D_c} \right) \quad (14)$$

with $\hat{u}(k) = \mathcal{S}(\bar{u})$ computed by the saturation function of Eq. (3). The PID controller state evolution is given by rewriting Eq. (14) as

$$x_c(k+1) = \left(A_c - \frac{B_c C_c}{D_c} \right) x_c(k) + \frac{B_c}{D_c} \hat{u}(k). \quad (15)$$

Then, from Eq. (15), when $\bar{e}(k) \neq e(k)$ the PID is forced by a constant input given by $\hat{u}(k) = \{u_m, u_M\}$, such that the controller state vector and the output are not directly driven by the feedback error. Furthermore, according to Lemma 3.1, it is guaranteed that if the PID state does not influence the control output for any value of $e(k)$, such that the control effort is computed by

$$\bar{u} = C_c x_c(k) + D_c \left(\frac{\hat{u}(k)}{D_c} - C_c x_c(k) \frac{1}{D_c} \right) = \hat{u}(k). \quad (16)$$

Eq. (16) shows the proposed EG policy computes the managed error such that the constrained input is not directly related to the PID state vector evolving according to Eq. (14) or to the PID model of Eq. (4). Then, the windup issue does not affect the PID controller because of the introduction of the EG algorithm in the closed-loop system. Note, because the EG action affects the full PID state variables, it could be used also to limit the effect of other common PID loop issues, e.g. the derivative backoff (Theorin & Hägglund, 2015).

3.5. Error governor algorithms

In this section the proposed EG algorithms, based on the solution of the QP problem of Eq. (9) and on the efficient solution given by Lemma 3.1 are reported, considering the control scheme of Fig. 1.

Algorithm 1 Optimal EG Algorithm

Input: Feedback error $e(k)$, PID state $x_c(k)$, QP problem matrices H, F, G, W, w

- 1: **if** $k = 0$ **then**
 - 2: $x_c(k) = x_c(0);$ ▷ State vector initialization
 - 3: **end if**
 - 4: $\rho_k \leftarrow [e(k), x_c(k)]';$
 - 5: $z^* \leftarrow \min_z \frac{1}{2} z' H z + \rho_k' F' z$ s.t. $Gz \leq W\rho_k + w;$
 - 6: $\bar{e}(k) \leftarrow z^*;$
 - 7: $x_c(k+1) \leftarrow A_c x_c(k) + B_c \bar{e}(k);$ ▷ State vector update
-

Output: The governed error $\bar{e}(k)$ to be applied to the PID controller.

Remark 2. The PID controller dynamics computed according to Eq. (5) is deterministic and, considering the PID state-space form as in Eq. (4), the initial value of state vector $x_c(0)$ is a-priori known.

According to the optimal EG policy and the efficient EG solution presented in Sec. 3.2 and Sec. 3.3, the implicit and the efficient version of the EG algorithm are proposed in Algorithm 1 and Algorithm 2, respectively. Due to Remark 2, in a real-world application the initial value of the PID integrator and derivative variables is known a-priori. Proposing the EG policy as an add-on solution to introduce in provided closed-loop systems, both the proposed formulations of the algorithm consider an internal update of the PID state variable, avoiding any kind of change or communication among the provided PID and the introduced EG.

Algorithm 1 proposes the implicit formulation of the EG algorithm, requiring a QP solver to compute the optimal value of the managed error $\bar{e}(k)$ in order to satisfy the PID control effort bounds. This version of the algorithm represents the base-version of the EG. Due to the time-consuming operation of solving the EG QP, the use of this algorithm could be limited to low control rate plants, when the control board resources permit to efficiently solve a constrained quadratic programming problem without introducing delays in the provided PID control loop.

Algorithm 2 considers the efficient solution of the EG algorithm, as presented in Sec. 3.3. This version of the algorithms requires the development of the saturation function of Eq. (3), used to compute the managed error value when a PID control

input constraint is active. This algorithm, with respect to the version given in Algorithm 1, does not require the introduction of a QP solver, drastically reducing the time execution and the computational burden required to solve the constrained optimization problem, overcoming practical limitation related to Algorithm 1. Furthermore, according to Lemma 3.1, the EG action computed by Algorithm 2 is equivalent to the managed error obtained by the implicit EG policy of Algorithm 1.

Algorithm 2 Efficient Optimal EG Algorithm

Input: Feedback error $e(k)$, PID state $x_c(k)$, PID parameters spaces-state matrices A_c, B_c, C_c, D_c , control input bounds u_m, u_M

- 1: **if** $k = 0$ **then**
 - 2: $x_c(k) = x_c(0);$ ▷ State vector initialization
 - 3: **end if**
 - 4: $\Delta_x \leftarrow C_c x_c(k);$
 - 5: $\tilde{u} \leftarrow \Delta_x + D_c e(k);$
 - 6: $\hat{u}(k) \leftarrow \mathcal{S}(\tilde{u});$ ▷ See Eq. (3)
 - 7: $\bar{e}(k) \leftarrow (\hat{u}(k) - \Delta_x) D_c^{-1};$
 - 8: $x_c(k+1) \leftarrow A_c x_c(k) + B_c \bar{e}(k);$ ▷ State vector update
-

Output: The governed error $\bar{e}(k)$ to be applied to the PID controller.

3.6. Computational complexity

Here an analysis of the computational burden related to proposed EG is presented.

Remark 3. Given two matrices $A \in \mathbb{R}^{n \times m}$ and $B \in \mathbb{R}^{m \times p}$, the matrix product $C = A \cdot B$ is computed by performing $m \cdot p \cdot n$ multiplications and $m \cdot p \cdot (n - 1)$ additions, such that the number of floating point operations (FLOPs) c required to compute the matrix $C \in \mathbb{R}^{n \times p}$ is $c = m \cdot p \cdot (2n - 1)$.

Considering the complexity of a matrix multiplication computed according to Remark 3 and the state-space formulation of the PID controller given in Eq. (6), the number of FLOPs performed to compute the PID control action is $c_{PID} = 17$ given by

$$c_{PID} = (n_{x_c} + n_y) [(2n_{x_c} - 1) + (n_u - 1)] + 2(n_{x_c} + n_u). \quad (17)$$

The proposed Algorithm 1 solves a constrained QP problem, requiring a computational complexity that can be studied by different algorithms (Cimini & Bemporad, 2017). On the other side, the computational burden required to execute the efficient EG of Algorithm 2 is computed directly according to Remark 3, such that the proposed EG introduces in the PID control loop an additional complexity of $c_{EG} = 7$ FLOPs. The overall computational complexity c_{FB} of the feedback law given by EG and PID policies is then efficiently calculated, such that $c_{FB} = c_{PID} + c_{EG} = 24$ FLOPs.

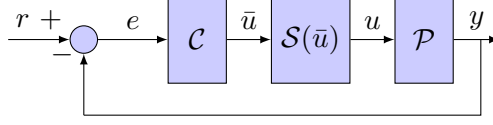


Figure 2. Closed-loop system with saturation

3.7. Stability Analysis

Defining the extended state vector

$$\xi(k) = [x_c(k) \quad x(k)]' \in \mathbb{R}^{n_{x_c} + n_x} \quad (18)$$

and the matrices

$$\tilde{A} = \begin{bmatrix} A_c & -B_c C_p \\ B_p C_c & A_p - B_p D_c C_p \end{bmatrix} \quad (19)$$

$$\tilde{B} = \begin{bmatrix} B_c \\ B_p D_c \end{bmatrix} \quad (20)$$

$$\tilde{C} = [\bar{0} \quad C_p] \quad (21)$$

$$\tilde{K} = \begin{bmatrix} \bar{0} \\ -B_p \end{bmatrix} \quad (22)$$

$$K = [C_c \quad -D_c C_p] \quad (23)$$

and the function

$$\psi(v) = v - \mathcal{S}(v) \quad (24)$$

the closed loop system without EG (see Fig. 2) is

$$\begin{aligned} \xi(k+1) &= \tilde{A}\xi(k) + \tilde{B}r(k) + \tilde{K}\psi(K\xi(k) + D_c r(k)) \\ y(k) &= \tilde{C}\xi(k) \end{aligned} \quad (25)$$

Assumption 1 Pairs (A_p, B_p) and (C_p, A_p) are assumed to be controllable and observable, respectively.

Adding the reference governor, in the case of SISO systems and PID controllers, the matrix \tilde{K} changes in

$$\bar{K} = \tilde{K} + R = \tilde{K} + \begin{bmatrix} -\frac{B_c}{D_c} \\ 0 \end{bmatrix} \quad (26)$$

the closed loop system with EG (see Fig. 1) is

$$\begin{aligned} \xi(k+1) &= \tilde{A}\xi(k) + \tilde{B}r(k) + \bar{K}\psi(K\xi(k) + D_c r(k)) \\ y(k) &= \tilde{C}\xi(k) \end{aligned} \quad (27)$$

In the following, we assume that the external input $r(k) = 0$ and we study the behavior of the unforced system. In the absence of control bounds (i.e., saturation nonlinearity), if the matrix \tilde{A} is supposed to be Hurwitz, then the closed-loop system is globally stable.

By definition, $\psi(K\xi(k))$ is a decentralized deadzone nonlinearity and satisfies the following sector condition $\psi(K\xi(k))' [\psi(K\xi(k)) - \lambda K\xi(k)] \leq 0$, $\forall \xi \in S(K, u_0^\lambda)$, where λ is a positive value (see Tarbouriech (2014), Khalil (1992)).

Definition 1 A set \mathcal{E} is said to be a region of asymptotic stability for the system (27), if $\forall \xi(0) \in \mathcal{E}$ the corresponding trajectory converges asymptotically to the origin. Considering the following Lyapunov candidate function

$$V(\xi(k)) = \xi(k)' P \xi(k), \quad P = P' > 0 \quad (28)$$

Theorem 1 If there exists a symmetric positive definite matrix $W \in \mathbb{R}^{(n_{x_c} + n_x) \times (n_{x_c} + n_x)}$ and positive scalars λ, ρ satisfying:

$$\begin{bmatrix} -W & \lambda W K' & W \tilde{A}' \\ \lambda K W & -2 & \tilde{K}' + R' \\ \tilde{A} W & \tilde{K} + R & -W \end{bmatrix} < 0 \quad (29)$$

$$\begin{bmatrix} W & (\lambda - 1) W K' \\ (\lambda - 1) K W & \rho u_0^2 \end{bmatrix} \geq 0 \quad (30)$$

$$0 < \lambda \leq 1 \quad (31)$$

then the ellipsoid $\mathcal{E}(P, \rho^{-1}) = \{\xi \in \mathbb{R}^{n_{x_c} + n_x}, \xi' P \xi \leq \rho^{-1}\}$, with $P = W^{-1}$, is a region of stability for the system (27). The satisfaction of relations (30) implies that the set $\mathcal{E}(P, \rho^{-1})$ is included in the set $S(K, u_0^\lambda)$ (see Gomes da Silva, Paim, and Castelan (2001), da Silva and Tarbouriech (2004)).

Proof By considering the quadratic candidate Lyapunov function as defined in (28) and by computing $\Delta V(\xi)$ along the trajectories of system (27) with $r(k) = 0$, we get:

$$\Delta V(\xi) = V(\xi(k+1)) - V(\xi(k)) = \xi(k+1)' P \xi(k+1) - \xi(k)' P \xi(k) = \quad (32)$$

$$= \left(\tilde{A} \xi(k) + \tilde{K} \psi(K \xi(k)) \right)' P \left(\tilde{A} \xi(k) + \tilde{K} \psi(K \xi(k)) \right) - \xi(k)' P \xi(k) \quad (33)$$

Since $-2\psi(K\xi(k))' [\psi(K\xi(k)) - \lambda K\xi(k)] \geq 0$, its addition to the right-hand side of the last equality gives an upper bound on $\Delta V(\xi)$. Therefore

$$\Delta V(\xi) \leq \Delta V(\xi) - 2\psi(K\xi(k))' [\psi(K\xi(k)) - \lambda K\xi(k)] \quad (34)$$

$$\Delta V(\xi) \leq \begin{bmatrix} \xi(k)' & \psi(K\xi(k))' \end{bmatrix} M \begin{bmatrix} \xi(k) \\ \psi(K\xi(k)) \end{bmatrix} \quad (35)$$

where

$$M = \begin{bmatrix} \tilde{A}'P\tilde{A} - P & \tilde{A}'P\tilde{K} + \lambda K' \\ \tilde{K}'P\tilde{A} + \lambda K' & \tilde{K}'P\tilde{K} - 2I \end{bmatrix} \quad (36)$$

By left- and right-multiplying the matrix (29) for $\text{Diag}(P, 1, I)$, where $P = W^{-1}$, we obtain

$$\begin{bmatrix} -P & \lambda K' & \tilde{A}' \\ \lambda K & -2 & \tilde{K}' \\ \tilde{A} & \tilde{K} & -P^{-1} \end{bmatrix} \quad (37)$$

Since (37) is a symmetric matrix, by using Schur's complement, we obtain that (37) is negative definite if and only if

$$-P^{-1} < 0 \quad (38)$$

$$\begin{bmatrix} -P & \lambda K' \\ \lambda K & -2 \end{bmatrix} - \begin{bmatrix} \tilde{A}' \\ \tilde{K}' \end{bmatrix} (-P) \begin{bmatrix} \tilde{A} & \tilde{K} \end{bmatrix} < 0 \quad (39)$$

where the first inequality is satisfied if W is a positive definite matrix and, since the left-side of the second inequality is equal to M , the second inequality is satisfied if $M < 0$. We can conclude that $\Delta V(\xi) < 0$ if (29) is satisfied (i.e., $M < 0$). Since this reasoning is valid $\forall \xi(k) \in \mathcal{E}(P, \rho^{-1})$, $\xi(k) \neq 0$, it follows that the function $V(\xi(k))$ is strictly decreasing along the trajectories of system (27). Hence, we can conclude that $\mathcal{E}(P, \rho^{-1})$ is a stability region for system (27) which means that $\forall \xi(0) \in \mathcal{E}(P, \rho^{-1})$, the corresponding trajectory converges asymptotically to the origin.

Corollary If there exists a symmetric positive definite matrix $W \in \mathbb{R}^{(n_{xc}+n_x) \times (n_{xc}+n_x)}$ satisfying:

$$\begin{bmatrix} -W & WK' & W\tilde{A}' \\ KW & -2 & \tilde{K}' + R' \\ \tilde{A}W & \tilde{K} + R & -W \end{bmatrix} < 0 \quad (40)$$

then the origin is globally asymptotically stable for the saturated system (27). In this case, the nonlinearity $\psi(K\xi(k))$ satisfies the sector condition $\forall \xi \in \mathbb{R}^{n_{xc}+n_x}$, i.e., the region $S(K, u_0^\lambda)$ corresponds to the whole state space.

Stability analysis for more general conditions, i.e., MIMO systems, generalized sector condition, continuous time systems can be find in da Silva and Tarbouriech (2005), da Silva and Tarbouriech (2004), Tarbouriech (2014).

4. Simulation Studies

In this section different simulation examples are considered to evaluate the performance of the proposed algorithm. The first and the second examples consider the control of a first order plus time delay (FOPTD) system and a second-order underdamped plant (SOUNP), proposed in (Pannocchia, Laachi, & Rawlings, 2005). Considering a

Table 1. Simulations Test Integral Square Error Results

Model	ISE _S	ISE _{SW}	ISE _{EG}
FOPTD	44.6560	47.7206	40.5834
SOUP	65.2124	139.6489	32.4220
EFM	12.54×10^6	9.49×10^6	8.58×10^6

real-world case study, from (Hodel & Hall, 2001) the control of an electric furnace model (EFM) with input saturation is proposed in the third example. In reported simulation studies, the proposed EG scheme has been used for imposing saturation constraints on the PID controllers. Note, the use of the EG on saturated or not saturated PID provides common performance, and in the proposed study the governor has been used to impose constraints on the controller without input saturation. The PID with EG control performance has been compared with respect to PID controllers with saturation, with and without anti-windup action. The anti-windup method considered for avoiding the windup effect on PID controllers is the tracking back-calculation scheme (Astrom & Hagglund, 2005; Li, Park, & Shin, 2011). Reported figures use the subscript *EG* for indicating results given by introducing the proposed EG scheme in the PID control loop, *S* for the PID with control input saturation and *SW* for the PID with saturation and anti-windup action. Simulation results are evaluated in terms of the Integral Square Error (ISE) performance index, provided by the PID working in conjunction with the EG (ISE_{EG}), the PID with saturation (ISE_S) and the PID with saturation and anti-windup (ISE_{SW}). These results, presented and compared for each case-study, are summarized in Table 1.

4.1. First-order plus time delay plant

In the first example, the first-order plus time delay plant, described in (Pannocchia et al., 2005), is presented. The continuous-time transfer function of the plant is

$$G(s) = \frac{e^{-2s}}{10s + 1} \quad (41)$$

The discrete transfer function using the zero-order hold as discretization method is

$$G(z) = z^{-2/T_s} \frac{0.02469}{z - 0.9753} \quad (42)$$

The controller is designed considering a sample time $T_s = 0.25$ s and introducing the control input saturation, such that $u_M = -u_m = 1.5$. The PID controller is designed in parallel form according to Eq. (5), with tuning parameters $K_p = 2.51$, $K_i = 0.1451$, $K_d = 0$ computed by the Skogestad IMC method (Skogestad, 2003). The controlled system has been tested also by introducing two external disturbance steps of 5 s, at time 50 s and 170 s of amplitude -1 and $+1$, respectively. Figure 3 shows the controlled outputs, the control signals and the feedback errors for the three controllers, the PID with and without anti-windup action and with EG. The control performance have been evaluated considering a set of step responses, forcing the control signal to saturate according to the control effort bounds. Compared with respect to the saturated PID, the introduced EG algorithm allows to reduce the overshoot, related to the integrator windup issue affecting the controller. Considering the PID featured

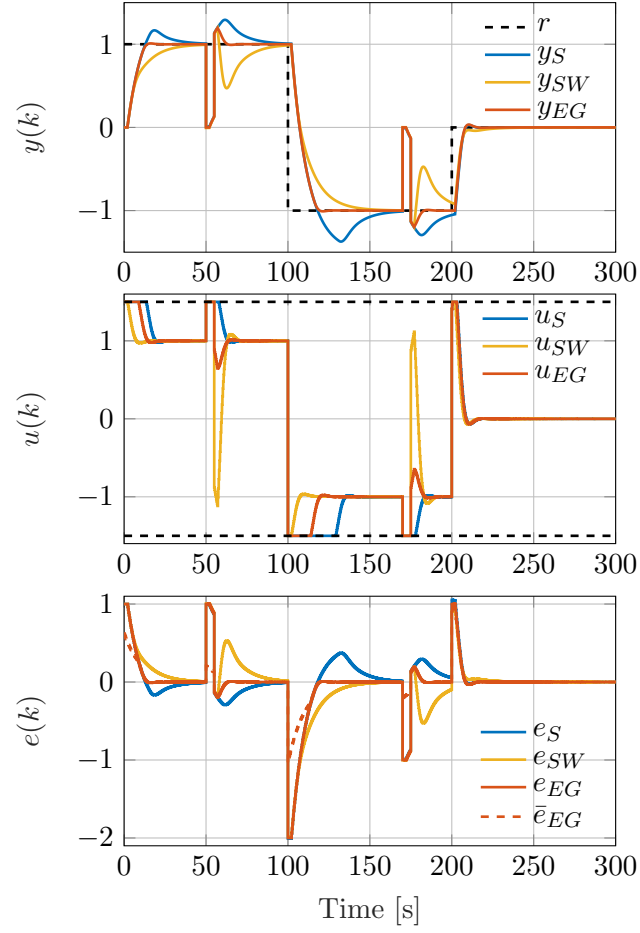


Figure 3. First-order plus time delay plant comparison results. From top to bottom: the controlled outputs (solid lines) together with the reference signal (dashed line); the control signals (solid lines) together with the saturation bounds (dashed lines); the feedback errors (solid lines) together with the managed error (dashed line).

by the anti-windup action, the presented EG permits to maintain the linear control law performance of the nominal PID until the output reaches the saturation value, improving the transient response and neglecting the windup problem. Whereas, when the saturation is not reached, the PID controller with EG performs the nominal PID control. The improvement given by EG is shown also verifying the ISE values collected in Table 1, with respect to the overall presented simulations. Compared with the performance of the PID working in conjunction with EG, the standard saturated PID with and without anti-windup action causes an increasing of the ISE value of +10.04% and +17.59%. Note, introduction of the anti-windup action causes a slower closed-loop response but permits to avoid any overshoot of the controlled output, instead of the saturated PID.

4.2. Second-order underdamped plant

The second example considers the second order underdamped plant also given in (Pannocchia et al., 2005). The continuous-time transfer function of the plant is

$$G(s) = \frac{K}{\tau^2 s^2 + 2\tau\xi s + 1} \quad (43)$$

with $K = 1$, $\tau = 5$ and $\xi = 0.2$. The discrete transfer function using the zero-order hold as discretization method is

$$G(z) = \frac{0.001241z + 0.001233}{z^2 - 1.978z + 0.9802} \quad (44)$$

Again, the PID has been calibrated by the Skogestads IMC method, with sample time $T_s = 0.25$ s and input saturation $u_M = -u_m = 1.5$. Controller tuning parameters are $K_p = 0.4$, $K_i = 0.2$, $K_d = 5$ and $\delta = 1$. As, for the previous example, the controlled system has been tested also by introducing two external disturbance steps of 5 s, at time 50 s and 170 s of amplitude -1 and $+1$, respectively. Figure 4 shows the controlled outputs, the control signals and the feedback errors for the PID with and without anti-windup action, and with EG. The performance of different control algorithms shows an increasing of the ISE value when the EG is replaced by alternative standard approaches. In particular, the PID with saturation increases the ISE of +101.14%, and the PID with anti-windup and saturation performs an ISE of +330.72% with respect to the PID with EG performance (see Table 1). Also in this case, the anti-windup action permits to reduce the amplitude of the overshoot, by providing a slower response in case of both input step reference signal and output disturbance. Furthermore, the EG permits to obtain better closed loop performance, reducing the issues given by the saturation and the way other policies faced it.

4.3. Electric furnace model

The third example considers the control of an electric furnace with bounded control input from (Hodel & Hall, 2001). The continuous-time state-space model of the furnace

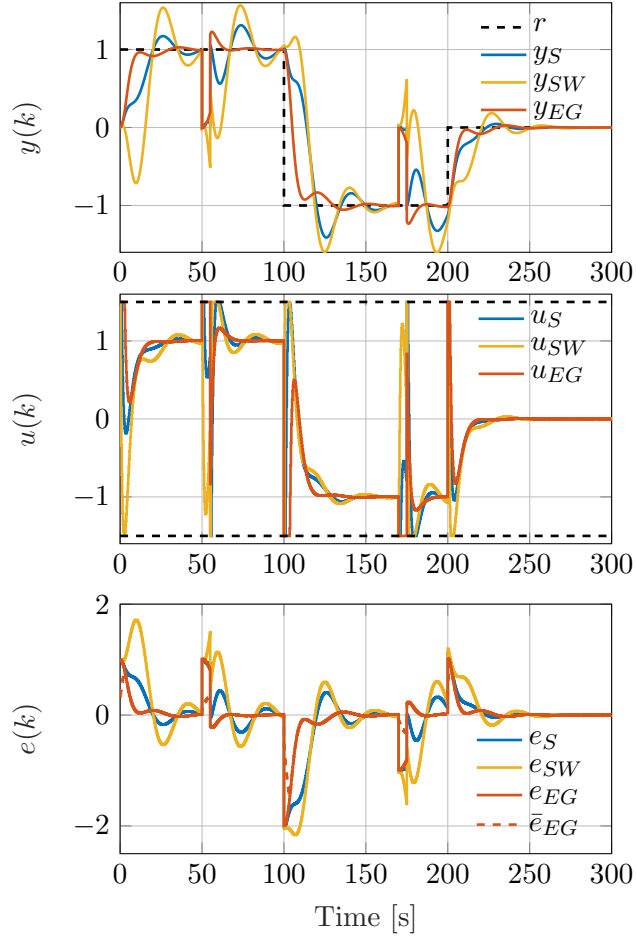


Figure 4. Second-order underdamped plant comparison results. From top to bottom: the controlled outputs (solid lines) together with the reference signal (dashed line); the control signals (solid lines) together with the saturation bounds (dashed lines); the feedback errors (solid lines) together with the managed error (dashed line).

is

$$\begin{aligned}\dot{x}(t) &= \begin{bmatrix} -0.02 & 0.02 \\ 0 & -1 \end{bmatrix} x(t) + \begin{bmatrix} 0 \\ 250 \end{bmatrix} u(t) \\ y(t) &= \begin{bmatrix} 1 & 0 \end{bmatrix} x(t)\end{aligned}\tag{45}$$

where the state vector is $x(t) = [c(t) \ f(t)]'$, with $f(t)$ the filament temperature and $c(t) = y(t)$ the chamber temperature to control. The discrete state space system using the zero-order hold as discretization method is

$$\begin{aligned}x(k+1) &= \begin{bmatrix} 0.9802 & 0.0125 \\ 0 & 0.3679 \end{bmatrix} x(k) + \begin{bmatrix} 1.826 \\ 158 \end{bmatrix} u(k) \\ y(k) &= \begin{bmatrix} 1 & 0 \end{bmatrix} x(k)\end{aligned}\tag{46}$$

The voltage control input $u(k)$ is constrained between $u_m = 0$ V and $u_M = 10$ V. The PID controller is tuned to compensate the system to be critically damped, with a settling time of 30 seconds, by setting $K_p = 0.16$, $K_i = 0.011$, $K_d = 0.13$, $\delta = 1.3667$ and sample time $T_s = 1$ s. Figure 5 shows the controlled outputs, the control signals and the feedback errors for the three controllers, PID with and without anti-windup action and with EG. Also in this last real world problem simulation results shown the effect of the EG policy introduced for working in conjunction with the PID controller. Considering the performance index presented in Table 1, the saturated PID, with and without anti-windup action, presents an increasing of the ISE of +46.15% and +10.61%, respectively, with respect to the closed-loop designed with PID and EG. This real world case-study permits to evaluate the effect of the EG on a common control problem. The EG permits to further reduce effects of the saturation, reducing overshoots related to both the PID tuning and saturation effects. The anti-windup, permitting a smooth output trajectory, causes a degradation of the control performance also for small changes in the output set-point. The EG does not present this behaviour, providing a closed loop response faster than the PID with saturation, but reducing the related overshoot.

5. Conclusions

This paper has proposed an optimal Error Governor (EG) for Proportional-Integral-Derivative (PID) controllers with input saturation. The aim is to improve the control performance of the standard PID with saturation, by managing the feedback error such that the computed control signal is bounded to the saturation limits. The algorithm considers to change the feedback error according to an optimal criteria, by solving a constrained Quadratic Programming (QP) problem. An approach for efficiently computing the solution of the QP is presented, permitting to apply the EG in those systems controlled by an high sampling frequency and/or low computational power boards. The application of the proposed EG on two academic examples and a real-world control problem, regarding the electric furnace control, is also presented. Tests have shown a remarkable improvements of the control performance by introducing the EG in a standard PID feedback loops when the controllers reach the saturation limits. Whereas, the EG does not affect the control action when it respects the saturation bounds, such that the PID provides the nominal behaviour. Simulations confirm

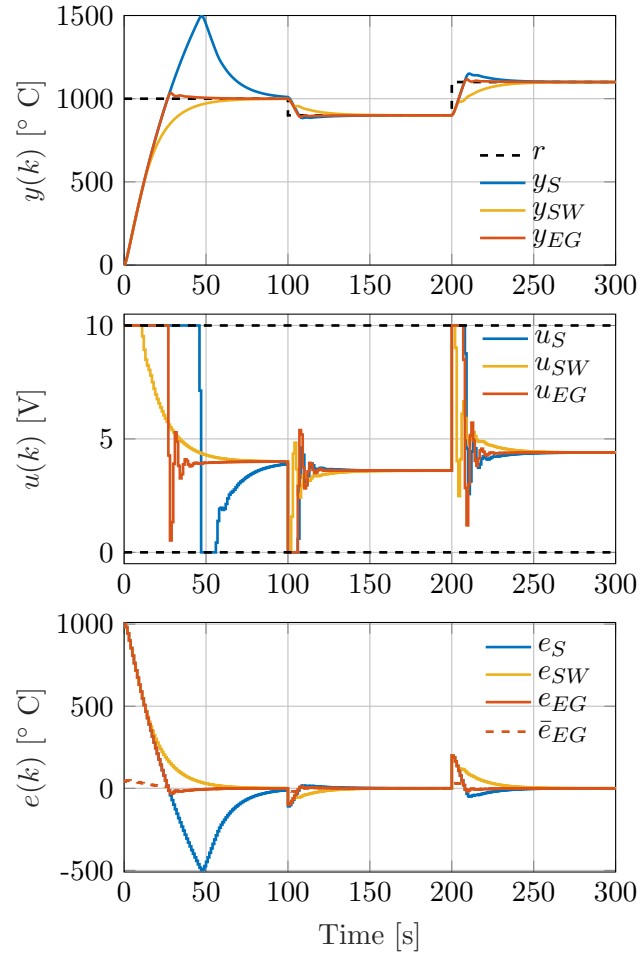


Figure 5. Electric furnace control comparison results. From top to bottom: the controlled outputs (solid lines) together with the reference signal (dashed line); the control signals (solid lines) together with the saturation bounds (dashed lines); the feedback errors (solid lines) together with the managed error (dashed line).

the high quality of the solution also comparing the Integral Square Error (ISE) index computed from the control results of the EG scheme with respect to the performance of PID provided of anti-windup action. Further development will consider the test of the proposed EG controlling a real plant and the development of an EG policy for nonlinear and multi-input multi-output (MIMO) controllers.

References

- Ang, K. H., Chong, G., & Li, Y. (2005). PID control system analysis, design, and technology. *IEEE transactions on control systems technology*, 13(4), 559–576.
- Angeli, D., & Mosca, E. (1999). Command governors for constrained nonlinear systems. *IEEE Transactions on Automatic Control*, 44(4), 816–820.
- Astrom, K., & Hagglund, T. (2005). Advanced PID control. research triangle park. NC 27709: *ISA-The Instrumentation, Systems, and Automation Society*.
- Åström, K. J., & Häggglund, T. (1995). *PID controllers: theory, design, and tuning* (Vol. 2). Instrument society of America Research Triangle Park, NC.
- Åström, K. J., & Häggglund, T. (2001). The future of PID control. *Control engineering practice*, 9(11), 1163–1175.
- Astrom, K. J., & Rundqwist, L. (1989). Integrator windup and how to avoid it. In *American control conference, 1989* (pp. 1693–1698).
- Azar, A. T., & Serrano, F. E. (2015). Design and modeling of anti wind up PID controllers. In *Complex system modelling and control through intelligent soft computations* (pp. 1–44). Springer.
- Bemporad, A. (1998). Reference governor for constrained nonlinear systems. *IEEE Transactions on Automatic Control*, 43(3), 415–419.
- Berner, J., Soltesz, K., Åström, K. J., & Häggglund, T. (2017). Practical evaluation of a novel multivariable relay autotuner with short and efficient excitation. In *IEEE Conference on Control Technology and Applications (CCTA), 2017* (pp. 1505–1510).
- Berner, J., Soltesz, K., Häggglund, T., & Åström, K. J. (2018). An experimental comparison of PID autotuners. *Control Engineering Practice*, 73, 124–133.
- Casavola, A., Franzè, G., Menniti, D., & Sorrentino, N. (2011). Voltage regulation in distribution networks in the presence of distributed generation: A voltage set-point reconfiguration approach. *Electric power systems research*, 81(1), 25–34.
- Cavanini, L., Cimini, G., & Ippoliti, G. (2016). Model predictive control for the reference regulation of current mode controlled dc-dc converters. In *IEEE 14th International Conference on Industrial Informatics (INDIN), 2016* (pp. 74–79).
- Cavanini, L., Cimini, G., & Ippoliti, G. (2017). A fast model predictive control algorithm for linear parameter varying systems with right invertible input matrix. In *25th Mediterranean Conference on Control and Automation (MED), 2017* (pp. 42–47).
- Cavanini, L., Cimini, G., Ippoliti, G., & Bemporad, A. (2017). Model predictive control for pre-compensated voltage mode controlled DC–DC converters. *IET Control Theory & Applications*, 11(15), 2514–2520.
- Cavanini, L., Colombo, L., Ippoliti, G., & Orlando, G. (2017). Development and experimental validation of a LQG control for a pre-compensated multi-axis piezosystem. In *IEEE 26th International Symposium on Industrial Electronics (ISIE), 2017* (pp. 460–465).
- Chaiyatham, T., & Ngamroo, I. (2017). Improvement of power system transient stability by PV farm with fuzzy gain scheduling of PID controller. *IEEE Systems Journal*, 11(3), 1684–1691.
- Cimini, G., & Bemporad, A. (2017). Exact complexity certification of active-set methods for quadratic programming. *IEEE Transactions on Automatic Control*, 62(12), 6094–6109.
- Cimini, G., & Bemporad, A. (2019). Complexity and convergence certification of a block principal pivoting method for box-constrained quadratic programs. *Automatica*, 100, 29–

- da Silva, J. M. G., & Tarbouriech, S. (2004). Anti-windup design with guaranteed regions of stability for discrete-time linear systems. In *Proceedings of the 2004 american control conference* (Vol. 6, p. 5298-5303).
- da Silva, J. M. G., & Tarbouriech, S. (2005). Antiwindup design with guaranteed regions of stability: an lmi-based approach. *IEEE Transactions on Automatic Control*, 50(1), 106-111.
- Ferreau, H. J., Almér, S., Verschueren, R., Diehl, M., Frick, D., Domahidi, A., ... Jones, C. (2017). Embedded optimization methods for industrial automatic control. *IFAC-PapersOnLine*, 50(1), 13194-13209.
- Garone, E., Di Cairano, S., & Kolmanovsky, I. (2017). Reference and command governors for systems with constraints: A survey on theory and applications. *Automatica*, 75, 306-328.
- Gomes da Silva, J. M., Paim, C., & Castelan, E. B. (2001). Stability and stabilization of linear discrete-time systems subject to control saturation. *IFAC Proceedings Volumes*, 34(13), 525 - 530. (1st IFAC Symposium on System Structure and Control 2001, Prague, Czechoslovakia, 27-31 August 2001)
- Hodel, A. S., & Hall, C. E. (2001). Variable-structure PID control to prevent integrator windup. *IEEE Transactions on Industrial Electronics*, 48(2), 442-451.
- Izadbakhsh, A., Kalat, A. A., Fateh, M., & Rafiei, M. (2011). A robust anti-windup control design for electrically driven robots theory and experiment. *International Journal of Control, Automation and Systems*, 9, 1005-1012.
- Izadbakhsh, A., & Kheirkhahan, P. (2018). Nonlinear pid control of electrical flexible joint robots-theory and experimental verification. In *IEEE International Conference on Industrial Technology (ICIT), 2018* (p. 250-255).
- Izadbakhsh, A., & Kheirkhahan, P. (2018). On the voltage-based control of robot manipulators revisited. *International Journal of Control, Automation and Systems*, 16, 1887-1894.
- Kahveci, N. E., & Kolmanovsky, I. V. (2010). Constrained control using error governors with online parameter estimation. In *49th IEEE Conference on Decision and Control (CDC), 2010* (pp. 5186-5191).
- Kapasouris, P., Athans, M., & Stein, G. (1988). Design of feedback control systems for stable plants with saturating actuators. In *Proceedings of the 27th IEEE Conference on Decision and Control* (p. 469-479 vol.1).
- Khalil, H. K. (1992). *Nonlinear systems; 1st ed.* Upper Saddle River, NJ: Prentice-Hall.
- Knospe, C. (2006). PID control. *IEEE Control Systems*, 26(1), 30-31.
- Kolmanovsky, I., Garone, E., & Di Cairano, S. (2014). Reference and command governors: A tutorial on their theory and automotive applications. In *American Control Conference (ACC), 2014* (pp. 226-241).
- Li, X.-l., Park, J.-G., & Shin, H.-B. (2011). Comparison and evaluation of anti-windup PI controllers. *Journal of Power Electronics*, 11(1), 45-50.
- Liu, G., & Daley, S. (2001). Optimal-tuning PID control for industrial systems. *Control Engineering Practice*, 9(11), 1185-1194.
- Mercader, P., Åström, K. J., Banos, A., & Hägglund, T. (2017). Robust PID design based on QFT and convex-concave optimization. *IEEE Transactions on Control Systems Technology*, 25(2), 441-452.
- Pannocchia, G., Laachi, N., & Rawlings, J. B. (2005). A candidate to replace PID control: SISO-constrained LQ control. *AIChE Journal*, 51(4), 1178-1189.
- Shi, C.-X., & Yang, G.-H. (2018). Robust consensus control for a class of multi-agent systems via distributed PID algorithm and weighted edge dynamics. *Applied Mathematics and Computation*, 316, 73-88.
- Skogestad, S. (2003). Simple analytic rules for model reduction and PID controller tuning. *Journal of process control*, 13(4), 291-309.
- Song, Y., Huang, X., & Wen, C. (2017). Robust adaptive fault-tolerant PID control of MIMO nonlinear systems with unknown control direction. *IEEE Transactions on Industrial Electronics*, 64(6), 4876-4884.
- Tarbouriech, S. (2014). *Stability and stabilization of linear systems with saturating actuators.*

- Springer Publishing Company, Incorporated.
- Tharayil, M., & Alleyne, A. (2002). Active supersonic flow control using hysteresis compensation and error governor. *IFAC Proceedings Volumes*, 35(1), 205–210.
- Theorin, A., & Hägglund, T. (2015). Derivative backoff: The other saturation problem for PID controllers. *Journal of Process Control*, 33, 155–160.
- Wang, H., Xiao, Z. W., Liu, H. B., & Liu, L. T. (2015). Multimode parameter fuzzy self-tuning pid precise temperature control system. In *Fifth Asia International Symposium on Mechatronics (AISM 2015)* (p. 1-4).